Marine Micropaleontology 126 (2016) 42–49

Contents lists available at ScienceDirect

Marine Micropaleontology

journal homepage: www.elsevier.com/locate/marmicro

Research paper

Zinc incorporation in the miliolid foraminifer *Pseudotriloculina rotunda* under laboratory conditions

M.P. Nardelli [a,b,*], D. Malferrari [c], A. Ferretti [c], A. Bartolini [d], A. Sabbatini [a], A. Negri [a]

[a] Department of Life and Environmental Sciences (DiSVA), Politechnic University of Marche, Ancona, Italy
[b] UMR CNRS 6112 LPG-BIAF, University of Angers, Angers, France
[c] Department of Chemical and Geological Sciences, University of Modena and Reggio Emilia, Modena, Italy
[d] Centre de Recherche sur la Paléobiodiversité et les Paléoenvironnements, UMR 7207 CNRS MNHN UPMC, Muséum National d'Histoire Naturelle, Paris Cedex 05, France

ARTICLE INFO

Article history:
Received 7 July 2015
Received in revised form 30 May 2016
Accepted 5 June 2016
Available online 06 June 2016

Keywords:
Foraminifera
Miliolid
Zn/Ca
LA-ICP-MS
Culture experiments
Pollution

ABSTRACT

The incorporation rate of Zn into the calcareous tests of *Pseudotriloculina rotunda* was investigated in culture in order to evaluate the possibility of using Zn/Ca ratios as a pollution proxy. Foraminifera were incubated at zinc concentrations up to 10-fold higher than unpolluted seawater (sea + 10 mg Zn/L) during 70 days. New calcite was investigated under the Environmental Scanning Electron Microscope (ESEM), for potential alteration of test structure. Laser ablation-Inductively Coupled Plasma-Mass spectrometry (LA-ICP-MS) was used to quantify Zn contents. The analyses revealed that test structure is not visibly altered by the presence of zinc. However, significant Zn incorporation is detected by the LA-ICP-MS. The zinc partition coefficient, D_{Zn}, decreases at increasing Zn concentrations (from 4.03 ± 0.06 to 0.2 ± 0.01) and the zinc is incorporated into the calcite not necessarily linearly.

1. Introduction

The recent worldwide legislation aims to restore the "pre-anthropic impacts" status in marine environments (e.g., WFD, 2000/60/EC and MSFD, 2008/56/EC in Europe). Information about the pristine faunas like those in pre-industrial times, however, are often impossible to obtain because of the scarcity (or lack) of reference stations that could still represent unimpacted present-day conditions. Fossilizing organisms represent an excellent historical archive of environmental conditions. Foraminifera are distributed worldwide in many different habitats, from brackish to marine, and their fossil records create an excellent historical archive which can be used as proxies for the reconstruction of past environments, such as pre-industrial ecological conditions (Schönfeld et al., 2012). A new approach involves the use of foraminiferal test geochemistry to assess the evolution of pollutant (i.e., metals) concentrations through time. Incorporation rates of trace elements are widely used as specific proxies in paleoceanography and paleoecology (e.g., Eggins et al., 2003; Hönisch and Hemming, 2005; Levi et al., 2007; Katz et al., 2010; Sabbatini et al., 2011), despite the possible bias linked to the biological influence on calcification processes (i.e., vital effects). The need to calibrate these proxies through culturing experiments was highlighted in the last decade by several authors (e.g., de Nooijer et al., 2007). This approach offers the advantage of changing one single variable (while all the others are kept constant) in order to better evaluate the vital effect. These biological aspects could be even more important for the incorporation rates of chemicals whose concentrations exceed natural baselines due to human activity, and that could be potentially used as pollution markers.

In this study we investigate the incorporation rates of Zn in the shell of the benthic miliolid foraminifer *Pseudotriloculina rotunda* (Schlumberger, 1893). Among foraminiferal species miliolids showed contradictory responses to heavy metal pollution in different studies. For example, decreasing miliolid relative abundances in polluted (by both organic and inorganic chemicals) coastal zones are reported and interpreted by some authors as a sensitivity index (e.g., Ferraro et al., 2006; Frontalini and Coccioni, 2008). Other studies, on the other hand, suggest a strong tolerance of several miliolid species to pollution, both in situ and under laboratory conditions (e.g., Samir and El-Din, 2001; Romano et al., 2008; Cherchi et al., 2009; Foster et al., 2012; Nardelli et al., 2013).

The aim of the present study is to calibrate incorporation rates of Zn in miliolid foraminiferal shells and thus evaluate the usefulness of the Zn incorporation rate as an environmental proxy. Zn is, in fact, one of the most common pollutants associated with human activities (e.g., Callender and Rice, 2000; Wuana and Okieimen, 2011), that can be toxic for biological systems when its concentration exceeds a threshold value (e.g., Haase et al., 2001; Valko et al., 2005; Díaz et al., 2006; Formigari et al., 2007). Nardelli et al. (2013) showed that inorganic Zn

* Corresponding author at: UMR CNRS 6112 LPG-BIAF, University of Angers, 2 Boulevard Lavoisier, 49045 Angers Cedex, France.
E-mail address: mariapia.nardelli@univ-angers.fr (M.P. Nardelli).

http://dx.doi.org/10.1016/j.marmicro.2016.06.001
0377-8398/

at concentrations higher than 0.1 mg/L can cause biological stress in *Pseudotriloculina rotunda*, causing delay in calcification rates.

In this regard, our study also aims to test the hypothesis that the biological stress caused by high Zn concentrations may influence metal incorporation rates as well. Zn incorporation was investigated using Laser Ablation Inductively Coupled Plasma Mass Spectrometer (LA-ICP-MS) analysis. Moreover, morphological observation using the Environmental Scanning Electron Microscope (ESEM) was employed to check for abnormalities in the organization/distribution of single shell crystallites. Nardelli et al. (2013) previously suggested that Zn does not cause macroscopic test deformations in miliolid foraminiferal shells, on the base of their observation of coiling patterns and chamber shapes of *P. rotunda* specimens grown at increasing zinc concentrations, under the binocular microscope. The aim of our ESEM analyses was to deepen these observations and check for calcite anomalies at the crystallite level.

2. Material and methods

2.1. Experimental set up

All the analyses were performed on specimens of *Pseudotriloculina rotunda* that grew at least one chamber during 70-days exposure to six different Zn concentrations under laboratory conditions. Zn-enriched solutions were prepared adding respectively 0.01, 0.1, 1.0, 10, and 100 mg/L of Zn to natural seawater (sea) from an unpolluted site (Portonovo, Adriatic Sea); Zn and Ca concentrations in natural seawater were measured using an Inductively Coupled Plasma Mass Spectrometer (ICP-MS). Although precautions were taken during manipulations, the ICP-MS analyses revealed that the zinc concentration of the natural seawater used for the experiment was higher than natural background. In fact the zinc concentration measured on culture waters before the addition of zinc was 0.149 ± 0.01 mg/L, while the zinc concentration of seawater from the sampling site was originally 0.237 ± 0.01 μg/L. However, as the same water was used to prepare all the zinc solutions for the different treatments and, considering the very high concentrations of added zinc, we believe that this contamination does not compromise the dataset. But, of course, this means that the lowest tested seawater zinc concentration of the experiment (named "sea" hereafter) cannot be considered as a control representative of unpolluted seawater conditions.

Temperature (15.0 ± 0.5 °C), salinity (38.0 ± 0.001) and pH (8.0 ± 0.1) were kept constant during the experiment. Refer to Nardelli et al. (2013) for further details on culture settings and preparation of Zn solutions.

As reported in Nardelli et al. (2013), none of the specimens produced new chambers at the highest tested Zn concentration (sea + 100 mg/L), therefore only specimens coming from culture sets from treatments sea, sea + 0.01, sea + 0.1, sea + 1 and sea + 10 mg/L were investigated. Moreover, two samples were treated for a "passive Zn incorporation test": empty tests of *P. rotunda* were exposed to sea + 10 mg/L Zn concentrations for two weeks in order to measure Zn passively adsorbed to calcite, without involving cellular-mediated mineralization processes.

2.2. ESEM and LA-ICP-MS sample preparation

The analyzed foraminiferal tests (n = 41) were washed with Millipore water and dried at 40 °C. The same cleaning procedure was performed on the two empty tests (n = 2) used for the passive incorporation test. To perform both ESEM observations and LA-ICP-MS analyses, samples were fixed to aluminium stubs using conductive carbon adhesive discs. All samples analyzed with an LA-ICP-MS were photographed under the ESEM before and after the analyses to check for the success of ablations (i.e., the correct chamber, no multiple chamber sampling, and no breakage of chambers – see Appendix, Fig. A.1a–c).

2.3. LA-ICP MS analysis: analytical protocol optimization

This study represents the first LA-ICP-MS investigation on miliolid foraminifera. Chemical composition, micro-structure and chamber arrangements of miliolids strongly differ from other benthic foraminifera more commonly analyzed with the LA-ICP-MS (i.e., Rotaliidae, e.g., de Nooijer et al., 2007; Munsel et al., 2010; Dissard et al., 2010; or Buliminidae, e.g., Hintz et al., 2006; Barras et al., 2010). Miliolid foraminifera have a calcareous non-lamellar imperforate test consisting of calcite needles randomly oriented in an organic matrix. They also possess a smoothly finished outermost layer of well crystallized calcite, with rhombohedral crystal faces arranged parallel to the surface (Debenay et al., 1998). Moreover, *Pseudotriloculina rotunda* creates chambers, each one-half coil in length, adding the new ones in planes oriented at 120°, with only three final externally visible chambers (Loeblich and Tappan, 1964).

For this reason it was necessary to optimize the existing protocols and to obtain the best ablation setting to be applied to our specimens. In particular, it was compulsory to prevent the laser from ablating the innermost (older) chambers. Several trials on foraminiferal tests were thus performed to find the most suitable combination of the instrument setting parameters. A detailed description of the followed procedures is given in Appendix A, and the values of the optimized parameter used for measurements are reported in Table 1. An example of successful sampling is shown in Fig. 1.

2.3.1. Analytical standards preparation and instrument calibration

A mass spectrometer, like any measurement device, requires a suitable calibration procedure. When laser ablation is employed, the interaction between laser and solid sample is complex and the response is dependent on the sample matrix. For this reason, two forms of calibration are mandatory: i) a reference (internal standard) is required to compensate for changes in the quantity of ablated mass, even when the concentration remains constant; ii) matrix-matched solid standards (frequently referred to as "external standards") are necessary to calibrate laser ablation processes and the instrument response. In fact, a relative measure of ablated mass can be achieved by simultaneously measuring emission from the analyte and a common matrix element (internal standard). For absolute calibration of the LA-ICP-MS conditions, standards made of the same matrix as the samples would be required, but are seldom available (e.g., Darke and Tyson, 1994; Raith et al., 1996; Hathorne et al., 2003).

Table 1
Optimized laser parameters. Linear ablation, carried out on the flatter part of the last chamber proceeding always from the center to the aperture of the chamber, was preferred to spot ablation. See Hathorne et al. (2003) for comparison and SI-1 for further information. A pre-ablation step was introduced to clean the surface from potential contaminations before data acquisition.

	Laser intensity (%)	Frequency (Hz)	Ablation line width (μm)	Duration (s)	Main results
Pre-ablation	10	1	55	230	Sampling only of external chamber, without crash
Ablation	50	4	55	230	Good signal intensity at the detector

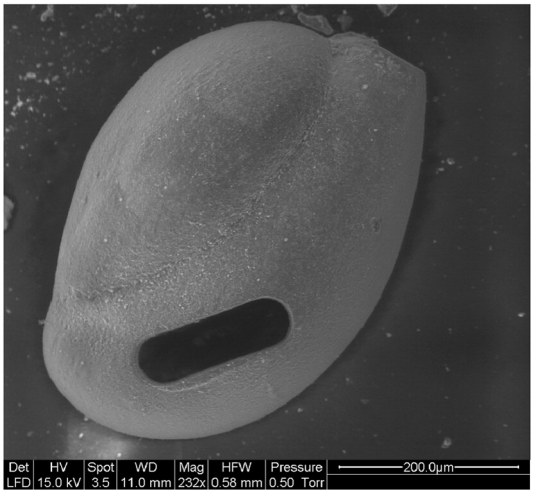

Fig. 1. Example of successful laser sampling on last chamber of *P. rotunda.*

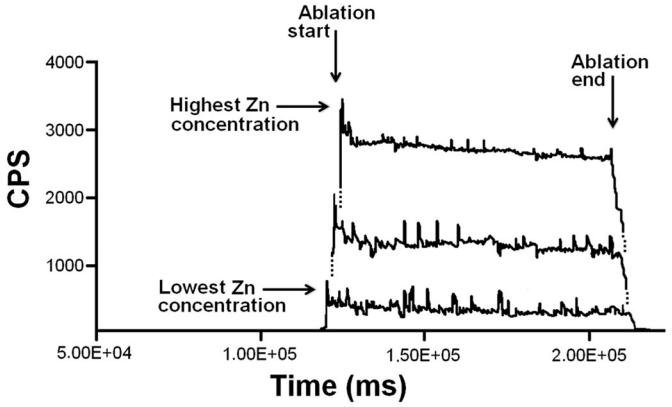

Fig. 2. Spectra resulting from the ablation lines measured on home-made standard Tablets at different Zn concentrations to verify if Zn distribution was homogeneous. The highest and the lowest curves represent the spectra measured respectively on 1050 ppm and 150 ppm zinc home-made standards. CPS means counting per second.

Previous studies on perforate calcareous species of foraminifera (or other organisms with calcareous compounds) used NIST610-611 or NIST612-613 as external standards, together with internal standards (generally ^{44}Ca isotope) and "in-house made standards" (e.g., Hathorne et al., 2003; Eggins et al., 2003; Montagna et al., 2007; Rathmann and Kuhnert, 2008; Munsel et al., 2010). The same standards were also used in our study in order to test their possible employment also for miliolids. In-house made standards were obtained as hereafter described. Stock solutions with defined Zn concentration were prepared using Zn ICP-standard solutions [1 mg/mL in 2 (vol.%) HNO_3] and Millipore water. A proper amount of each solution was added to a mixture composed by 400 mg of ultrapure $CaCO_3$ powder (particle size less than 1 μm) and cellulose; to prevent $CaCO_3$ dissolution, the pH of each solution was adjusted to 7.5 ± 0.1 using an appropriate amount of ammonia solution. Each suspension was mixed and homogenized in an agate mortar and then dried at 30 °C for 12 h. The resulting powder was then re-homogenized in the agate mortar and pressed at 12 tons into tablets of 12 mm diameter. Such "standard tablets" at different Zn concentrations were then checked via LA-ICP-MS using ablation lines to verify whether Zn distribution was homogeneous. As shown in Fig. 2, the spectra resulting from these analyses revealed a fairly smooth plateau, confirming a homogeneous distribution of the element into the standard tablets.

According to the literature (see above), NIST standards could be used as well. However, the difference in composition of the matrix (i.e., silica glass in NIST standards, Ca carbonate in miliolids) does not match the second requirement mentioned above. However, several measurements using NIST610 were performed in order to test the possibility to use a certified and easily acquired analytical standard. In particular, the same laser parameters (i.e., the same ablation conditions) were applied to both NIST610 and our samples (miliolids) but the response on the internal standard (^{44}Ca) was not satisfactory (see next paragraph for more details).

In the light of these results, and also in agreement with Hathorne et al. (2003), only in house-made tablets were used as external standards for measurements here reported. In detail, nine in house made standards were used with Zn concentrations ranging from 0 (blank, $CaCO_3$ + cellulose + Millipore) to 1050 ppm.

2.4. LA-ICP-MS: analyses of samples and data elaboration

Eleven specimens from "sea", five from sea + 0.01 mg/L, six from sea + 0.10 mg/L, ten from sea + 1.0 mg/L, nine from sea + 10 mg/L, were analyzed by the LA-ICP-MS. Moreover, the two specimens for the "passive sorption tests" were investigated as well. In a few cases more than one ICP-MS analysis was carried out on the same chamber, otherwise one linear ablation per chamber was generally realized. Standards were ablated using exactly the same laser setting parameters used for foraminifera, and their concentrations were regularly measured during sampling procedure, in order to correct instrumental deviation.

^{66}Zn and ^{68}Zn isotopes, and ^{44}Ca were measured. Collision mode using a mixture of helium (95%) and hydrogen (5%) was employed to discriminate the analyte ions from any interfering polyatomic ions on the basis of Kinetic Energy Discrimination (KED). Both for calibration and for sample measurements, Ca and Zn concentrations were calculated integrating over a time-interval of 1.00E + 05 ms in the flattest region of each spectrum of each individual ablation profile using PlasmaLab™ Software Package 2007.

For data analyses the relation between Zn/Ca ratios in calcite and seawater was observed. Partition coefficients for Zn were calculated for each set of Zn enriched cultures following the formula $D_{Zn} = (Zn/Ca_{calcite})/(Zn/Ca_{seawater})$.

3. Results

3.1. ESEM observations

Results from ESEM observations on structure and crystal organization of Zn-exposed foraminiferal tests did not reveal any obvious anomalies. All specimens showed the typical structure of miliolid tests (Fig. 3a–d), characterized by organized crystals on the external test surface and disorganized crystals in an organic matrix in the inner part of the wall (Hay et al., 1963; Towe and Cifelli, 1967; Haake, 1971; Debenay et al., 1998).

ESEM observations were also performed to adjust laser ablation parameters (see Appendix A) and to check samples for correct ablation after LA-ICP-MS measurements.

3.2. LA-ICP-MS measurements

The main results of the LA-ICP-MS analysis are given in Fig. 4(a, b). The Zn seawater concentrations are given in Zn/Ca mmol/mol to facilitate the comparison with Zn/Ca ratios in the calcite. The different treatments (i.e., Zn concentrations) are indicated by the colors. The LA-ICP-MS analysis revealed that Zn/Ca ratio increases linearly with water concentrations at least up to sea + 1.0 mg/L (Fig. 4b). The Zn/Ca shell concentrations vary between 1.11 ± 0.02 mmol/mol for the "sea" treatment and 1.77 ± 0.04 mmol/mol of the treatment sea + 1.0 mg/L (Table 2; see also Table A.2 in Appendix A for the complete dataset). The measurements obtained on calcite produced at the highest tested Zn concentrations (sea + 10 mg/L), however, with average Zn/Ca values

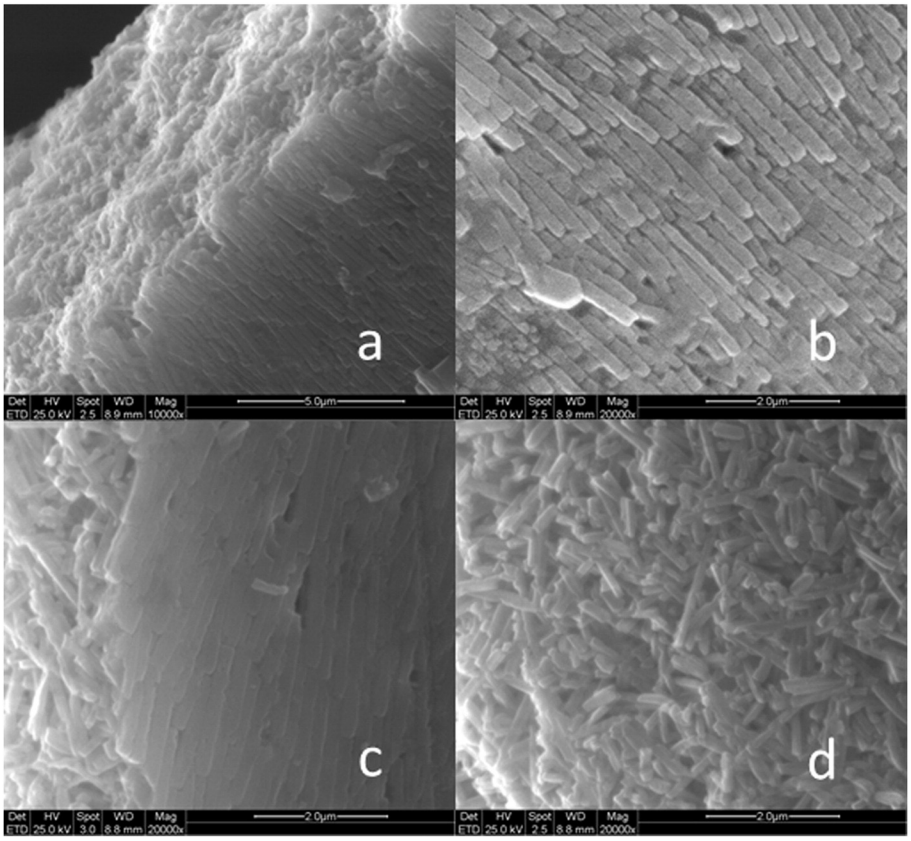

Fig. 3. ESEM micrographs of *P. rotunda*'s test. a) View of external wall of a specimen from "sea" treatment; b) detail of crystals on the external wall of the same specimen; c) View of external wall of a specimen from sea + 10 mg Zn/L contaminated cultures and d) detail of internal part of the wall, with disorganized crystals of the same specimen.

of 3.81 ± 0.17 mmol/mol, suggest the possibility that the linear trend, observed for seawater Zn concentrations lower than sea + 1.0 mg/L, can turn towards a plateau for higher concentrations. Possible explanations of this trend are discussed later.

The passive sorption test on empty shells incubated at sea + 10 mg/L conditions showed very low Zn concentrations ($Zn/Ca_{calcite}$ = 1.17 ± 0.01 mmol/mol), comparable to the ones of samples from the "sea" treatment) ($Zn/Ca_{calcite}$ = 1.12 ± 0.02 mmol/mol), and more than 3 times lower than living samples from highest tested zinc concentrations (sea + 10 mg/L) ($Zn/Ca_{calcite}$ = 3.83 ± 0.17 mmol/mol) (Fig. 4 and Table A.2 of Appendix A).

The calculated Zn partition coefficients (D_{Zn}) for each Zn treatment (indicated by the colors) are given in Fig. 5a. The average D_{Zn} (± standard deviation) is given in numbers. Because of non-homogeneous

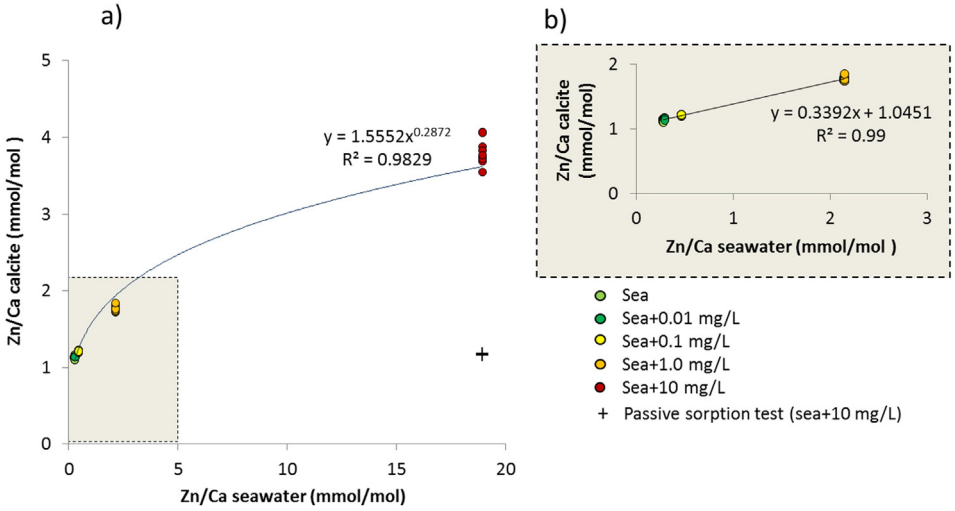

Fig. 4. Zn/Ca ratios in *Pseudotriloculina rotunda* calcite in function of Zn/Ca in seawater. a) All the samples are included (the colors correspond to the different Zn treatments). The best fitting of power function to predict $(Zn/Ca)_{calcite}$ to $(Zn/Ca)_{seawater}$ relationship is shown in blue and compared to the linear model (black dashed line). b) This is an enlargement of the left corner of Fig. 4a where the lower Zn/Ca points are shown separately.

Table 2
Mean $Zn/Ca_{seawater}$, $Zn/Ca_{calcite}$ and D_{Zn} values (±standard deviations) for each Zn treatment.

Treatment	$Zn/Ca_{seawater}$ (mmol/mol)	$Zn/Ca_{calcite}$ (mmol/mol) (±s.d.)	D_{Zn} (±s.d.)
Sea	0.278	1.122 (±0.028)	4.034 (±0.059)
Sea + 0.01 mg Zn/L	0.297	1.152 (±0.012)	3.880 (±0.042)
Sea + 0.1 mg Zn/L	0.465	1.216 (±0.011)	2.616 (±0.024)
Sea + 1.0 mg Zn/L	2.145	1.771 (±0.037)	0.826 (±0.017)
Sea + 10.0 mg Zn/L	18.948	3.813 (±0.171)	0.201 (±0.009)

variance, the Kruskal-Wallis test and Mann-Whitney pairwise comparisons post-hoc test were performed to determine whether the difference between partition coefficients was significant among treatments (p-value < 0.001). The results showed that the Zn partition coefficients were all significantly different among treatments. The obtained average values of D_{Zn} varied between 4.03 ± 0.06 at "sea" conditions and 0.2 ± 0.01 at sea + 10 mg/L Zn concentration (Fig. 5) (total average D_{Zn} = 2.22 ± 1.56). The observed decrease of D_{Zn} at increasing seawater Zn concentration is well described by a power function (R^2 = 0.997; p-value < 0.001; see Fig. 5a). However, due to the difficulty to assess whether the results obtained for the highest tested concentration (sea + 10 mg/L) are affected by neglected precipitation of zinc oxides/hydroxides (see discussion paragraph 4.2) we reported in Fig. 5b only the D_{Zn} obtained at Zn treatments lower than this concentration. Even without the last concentration, the data are still well described by a power function (R^2 = 0.998; p-value < 0.001) and the regression equation slightly change from $y = 1.5552x^{-0.713}$ to $y = 1.4826x^{-0.775}$.

4. Discussion

4.1. ESEM structural observation of tests

Miliolids are often regarded as pollution sensitive organisms. Several studies on test deformity induced by environmental contamination suggest that miliolids are more easily affected by test deformities than other foraminifera. For example, Samir and El-Din (2001) found that the majority of deformed tests collected in the El-Mex Bay (Egypt) were miliolid shells. Also Sharifi et al. (1991) reported that deformed foraminiferal tests from the Southampton coastal area contained much higher Cu and Zn concentrations than non-deformed specimens, suggesting again a responsibility of these metals for test deformations. However, Nardelli et al. (2013) tested in laboratory conditions the biological effects of several Zn concentrations on *P. rotunda* and, despite the fact that some specimens calcified new chambers at Zn concentrations up to 10 mg/L, no obvious deformations due to Zn exposure were observed, in terms of chamber arrangements or general shape of the foraminiferal shells. Our ESEM observations confirm these results because the calcite produced during Zn exposure showed the typical aspect and arrangement known for the species (as described by Debenay et al., 1998). So, Zn exposure does not appear to be, by itself, a cause of abnormal calcification for *P. rotunda*, either at the macro or micro scale. A possible explanation for the fact that Zn is often found in anomalous tests is its possible covariance with other pollutants (for example other metals) or environmental parameters, which can be alone the real cause of test deformation or have synergic behaviors to zinc and enhance its toxicity (as demonstrated, for example, for Co and Zn by Bresson et al., 2013). In fact, even if Zn is one of the most cited heavy metals, potentially responsible for test deformation, many other pollutants and anthropogenic events were related to test deformities, e.g. Cd, Cr and Ti (Yanko et al., 1998), Cu (Le Cadre and Debenay, 2006), hydrocarbons and oil spills (e.g., Vénec-Peyré, 1981; Vénec-Peyré et al., 2010), rapid changes of salinity and hypersalinity (e.g., Eichler-Coelho et al., 1996; Sousa et al., 1997; Stouff et al., 1999; Geslin et al., 2002). The absence of visible test anomalies can be coherent with the hypothesis that Zn incorporation into biomineralized calcite may occur, as already observed on non-biogenic calcites (e.g., Elzinga and Reeder, 2000; Temmam et al., 2000), after substitution of Ca or Mg to form isomorphic Zn carbonates, as suggested by Madkour and Ali (2009).

4.2. Zinc incorporation

Despite the absence of deformations or visible abnormalities in the specimens analyzed in this study, high Zn/Ca contents were detected in the internal wall of the last chamber of the test by LA-ICP-MS analysis. The incorporation rates of Zn into the calcite do not seem to be constant at increasing Zn concentrations. Zn incorporation, in fact, linearly increases at lower concentrations (from sea to sea + 1.0 mg/L, Fig. 4b), but the measures obtained at Zn concentrations higher than sea + 1.0 mg/L, even if represented by the results from only one Zn treatment, suggest that at higher concentrations (i.e., sea + 10 mg/L) the trend determined at low concentrations (up to sea + 1.0 mg/L) is no longer respected (Fig. 4a). The decreasing Zn incorporation rate in

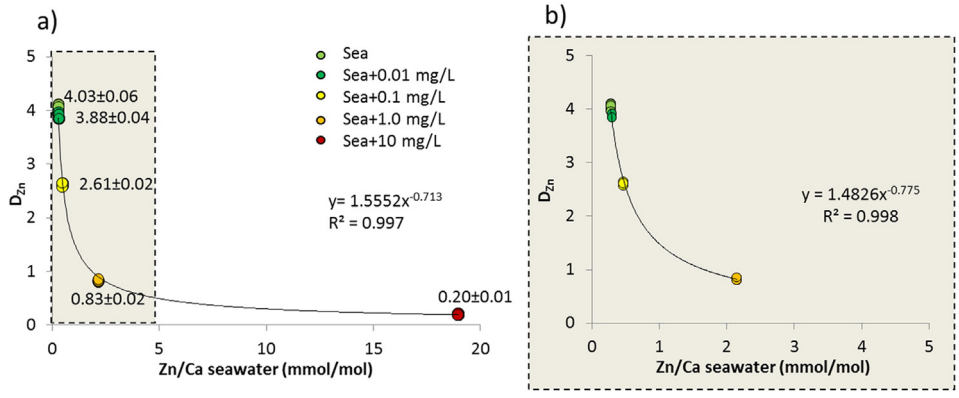

Fig. 5. Partition coefficients measured for each zinc treatment (the colors correspond to the different Zn treatments). The average D_{Zn} ± standard deviation for each treatment is given in numbers. a) All the D_{Zn} are included; b) D_{Zn} after exclusion of the sea + 10 mg/L treatment point. The corresponding regression curves, equations and R^2 are given for each dataset.

the shell is reflected by the partition coefficients that are lower for higher Zn seawater treatments (Fig. 5a, b).

Considering that we worked at high zinc concentrations we cannot avoid taking into account that zinc oxides/hydroxides precipitation could have been important at the highest zinc concentration we tested (sea + 10 mg/L). In fact, if we roughly estimate the expected Zn^{2+} saturation based on the pH of our cultures (8.0 ± 0.1) and neglect all potential influences of kinetics, we obtain a concentration of saturation of 4.37E-05 M, which is 3 times lower than the concentration of zinc we added to this treatment (see Table A.2 in Appendix A). Zinc oxides/hydroxides precipitation could therefore at least partially explain the decrease of Zn incorporation at sea + 10 mg/L condition.

However, this is not the first time that a similar decreasing trend for metal incorporation is observed on benthic foraminifera and this could be also partially due to biological reasons. For example Munsel et al. (2010) report similar observations for incorporated Ni in *Ammonia tepida*'s calcite. The incorporation of the metal is linear at low experimental concentrations and drops down when foraminifera are exposed to Ni concentrations 20-fold higher than natural seawater. The authors suggest that this could be due to biological effects. In fact, according to them, Ni at high concentrations could have toxic effects on foraminiferal cells and inhibit calcification. Toxic potential of some highly concentrated metals could trigger their cellular expulsion or blocking mechanism (for example metallothioneins-mediated) and prevent their incorporation in proportion to their sea water concentrations. This hypothesis is also valid for our study. Nardelli et al. (2013) reported delayed growth rates (i.e., calcification) of *Pseudotriloculina rotunda* exposed to Zn concentrations higher than sea + 1.0 mg/L and ascribed the reduced calcification rate to biological effects of high zinc concentrations on foraminiferal cell, invoking similar processes. Thus we think that the potential biological influence on the Zn incorporation observed at sea + 10 mg/L in the present study cannot be excluded. Some other possible explanations are hypothesized by Mewes et al. (2014) who also observed an exponential decreasing partition coefficient for Mg/Ca at increasing seawater metal concentrations following a power regression for two rotaliid foraminifera (*Ammonia aomoriensis* and *Amphistegina lessonii*): (a) presence of two different $CaCO_3$ layers, (b) involvement of two different biomineralization pathways. The first hypothesis depends on the possibility, shown for some foraminifera, to precipitate two different calcite phases, with two different Mg/Ca calcite ratios, independently of a migration of the foraminifera through different chemical environments (in the water column or in the sediment). This pathway was described by Bentov and Erez (2005) and particularly for *A. lessonii* and *Orbulina universa* by Branson et al. (2013). However, as far as we know, this biomineralization mechanism has not been described and does not fit with the existing calcification models for miliolid foraminifera. In fact the existing biomineralization models for miliolid foraminifera propose two main kinds of calcification mechanisms: miliolid foraminifera form bundles of oriented crystals into intracellular vesicles (e.g., Berthold, 1976; Angell, 1980) thanks to locally increased intracellular pH (de Nooijer et al., 2009). Each crystal is surrounded by an organic matrix, and bundles are passed through the cell membrane by exocytosis (e.g., Berthold, 1976; Hemleben et al., 1986). After exocytosis these crystals are accreted onto extracellular surfaces to form a packed wall structure (Hemleben et al., 1986).

The second hypothesis considers the involvement of different biomineralization pathways of Mg incorporation during calcification. This hypothesis derives from the biomineralization model proposed by Nehrke et al. (2013) for rotaliids foraminifera, but there is no evidence that the same processes occur in miliolid foraminifera. Therefore also this hypothesis does not seem to validly explain our results. Thus, the oversaturation of the highest tested zinc solution and/or the biological effect of potentially toxic zinc concentrations on the biomineralization process remain, to us, the more realistic hypothesis to explain the low zinc incorporation at sea + 10 mg/L treatment.

Apart from the exponential decrease of partition coefficient, another interesting point highlighted by our results is the apparent positive intercept of D_{Zn} ($Zn/Ca_{calcite}$ vs $Zn/Ca_{seawater}$) regression (Fig. 4b). This result suggests a difference in Zn incorporation for this miliolid species compared to all the rotaliid foraminifera for which D_{Zn} was previously estimated (e.g. Marchitto et al., 2000; Bryan and Marchitto, 2010). In fact, despite the highly variable D_{Zn} estimated for the different species, Marchitto et al. (2000) and Bryan and Marchitto (2010), report a $Zn/Ca_{calcite}$ vs $Zn/Ca_{seawater}$ regression line passing from the origin of the axes for all the measured rotaliids foraminifera. Similar results, showing a positive intercept on the y-axis, reported in Mewes et al. (2014) for Mg/Ca of two rotaliid foraminifera (*Ammonia aomoriensis* and *Amphistegina lessonii*), were hypothesized by the authors to be possibly due to purely chemical reasons: sorption of Mg^{2+} to mineral surfaces would be stronger than sorption of Ca^{2+} (Mucci and Morse, 1983) and then increased Mg^{2+} (adsorbed on calcite) would locally increase Mg/Ca, and then explain the positive y-axis intercept, especially at low seawater Mg/Ca. Due to its divalent nature and its ionic radii smaller than Ca^{2+}, this kind of mechanism is also possible for Zn^{2+} (Elzinga and Reeder, 2000). In this regard, the results of our sorption test (Fig. 4) seems to suggest that, at least at the highest tested concentration (sea + 10 mg/L), Zn sorption is negligible compared to the fraction incorporated into the calcite of living foraminifera incubated at the same Zn concentrations. This suggests that this kind of mechanism could have low influence on Zn enrichment of calcite. However, the test was performed only at the highest Zn treatment and it is not enough to draw any definitive conclusion about this aspect.

Another hypothesis, invoked by Langer et al. (2006) to explain the enriched Sr/Ca ratio in the calcite of the coccolithophore *Emiliania huxleyi*, could also explain the Zn/Ca enrichment we observe for *Pseudotriloculina rotunda*. Similarly to miliolid foraminifera, coccolithophores precipitate calcite into specific intracellular vesicles. According to the authors, the intracellular calcite precipitation yields an accumulation of Sr in the coccolith vesicle until Sr steady state is achieved. Then, the observed Sr/Ca of the coccolith calcite would be an integral value that arises from the sum of Sr/Ca over the time required for the formation of one coccolith. This is suggested to explain the enriched Sr/Ca ratios found in the coccolithophore compared to theorethical ones expected by purely chemical precipitation. According to us, and taking into account the results of our sorption test, this hypothesis seems more convincing to explain the apparent positive y-axis intercept of Fig. 4.

4.3. Implications for reconstructing past seawater zinc concentrations

As zinc is one of the most diffused pollutants related to the industrial activity (e.g., Callender and Rice, 2000; Wuana and Okieimen, 2011) a proxy for its concentrations in historical times could represent an important tool to study the evolution of marine ecosystems under anthropic stress. This is particularly interesting in view of the animated debates on the possible boundary for the recently proposed new epoch of the Anthropocene (e.g., Crutzen, 2002; Zalasiewicz et al., 2011). The accelerated increase of some industrial-derived pollutants is, in fact, one of the proposed points to establish the start of this epoch. Our results suggest a possible reliable identification and interpretation of one of these pollutants in the historical sediment record. In fact, except for the D_{Zn} estimated for the sea + 10 mg/L that could have been influenced by Zn oversaturation problems (as discussed above), we are confident that the D_{Zn} estimated for *Pseudotriloculina rotunda* in this study can be applied for past seawater concentrations reconstructions. The partition coefficients we obtained are different from the ones previously estimated for other foraminiferal species (mainly rotaliids), but rely on the variability range of values found for different species of rotaliid foraminifera (e.g. ~3 for *U. peregrina* to ~22 for *C. pachyderma* reported by Bryan and Marchitto, 2010) and they represent the Zn/Ca of the seawater where the calcite was biomineralized.

Zn/Ca contents into miliolid calcite could therefore allow reconstruction of concentrations of this metal in the past seawater.

The obtained D_{Zn} for each tested zinc concentrations (Fig. 5a) show statistically significant differences. For this reason we would suggest not to average all the values but rather using the equations given in Figs. 4b and 5b for Zn seawater reconstructions. For the highest tested zinc concentration, for which the estimated D_{Zn} could have been highly driven by zinc oxides/hydroxides precipitation and physiological cell problems due to potential toxic effects of zinc, our results are more difficult to apply and need further investigation to be confirmed. For the use of this proxy in potentially contaminated environments, the possible toxic effect of Zn at high concentrations on *P. rotunda* could be an important boundary constraint. A possible solution to overcome this problem could be the use of multiple species, with different thresholds of tolerance to zinc.

5. Concluding remarks

Zn/Ca ratios in calcite of *Pseudotriloculina rotunda* are a linear function of Zn/Ca in seawater at lower Zn/Ca seawater and appear to turn into a power function at Zn seawater concentrations higher than sea + 1.0 mg/L. Further studies are needed to quantify the possible influence of zinc oxides/hydroxides precipitation on the results we obtained at this higher experimental condition. However, even if we omit the last point from the dataset, the results show that Zn is incorporated in equilibrium with seawater concentrations and that partition coefficients significantly decrease at increasing seawater zinc concentrations following a power function. The result of passive sorption test performed on dead specimens incubated in water with high Zn concentration suggests that most of the zinc incorporation is mediated by the cell and that chemical passive sorption is putatively negligible (Table A.2). These results suggest the suitability of Zn/Ca into foraminiferal calcite as an environmental proxy. Zinc contents of calcite can be in fact considered representative of the concentrations in seawater at the time of their calcification, and relatively independent of post-mortem conditions occurring in the depositional area. The analysis of Zn/Ca contents into the calcite could therefore allow the reconstruction of past zinc concentrations in seawater. Then, present-day knowledge about tolerance limits of foraminifera (e.g., de Freita Prazeres et al., 2011; Nardelli et al., 2013) and other organisms to Zn seawater concentrations would allow us to study potential ecological effects induced by high concentrations of this metal in environmental systems in the past. However further studies would be needed for a more precise calibration of Zn/Ca as a proxy. In particular the study of potential synergic, additive or antagonistic effects of several chemicals and/or of environmental variables (e.g., salinity, temperature, alkalinity) on Zn incorporation should be deeply investigated. Moreover, further calibration will be very useful in the future to fill the gap for concentrations between 1 and 10 mg/L and between 0.1 mg/L and natural unpolluted seawater zinc concentrations (i.e., one order of magnitude lower).

Acknowledgements

The authors thank the reviewers, G.J. Reichart and an anonymous one for their important remarks and encouraging comments that strongly improved the manuscript. Thanks to the Polytechnic University of Marche (Italy) for funding the research. We thank the Centro Interdipartimentale Grandi Strumenti (CIGS) of the Università di Modena and Reggio Emilia (Italy) for the facilities and Daniela Manzini and Maria Cecilia Rossi for the technical support. Thanks to Dr. Silvia Illuminati and Prof. Scarponi for providing bottom seawater samples for background Adriatic seawater zinc concentration data. Many thanks to Christine Barras and Frans Jorissen for their valuable suggestions and discussions on a first draft of the manuscript.

Appendix A. Supplementary data

Supplementary data to this article can be found online at http://dx.doi.org/10.1016/j.marmicro.2016.06.001.

References

Angell, R.W., 1980. Test morphogenesis (chamber formation) in the foraminifer *Spiroloculina hyaline* schulze. J. Foraminifer. Res. 10, 89–101.
Barras, C., Duplessy, J.C., Geslin, E., Michel, E., Jorissen, F., 2010. Calibration of δ 18 O of laboratory cultured deep-sea benthic foraminiferal shells in function of temperature. Biogeosciences 7 (1), 1349–1356.
Bentov, S., Erez, J., 2005. Novel observations on biomineralization processes in foraminifera and implications for Mg/Ca ratio in the shells. Geology 33, 841–844.
Berthold, W.U., 1976. Biomineralisation bei milioliden Foraminiferen und die Matrizen-Hypothese. Naturwischenschaften 63, 196.
Branson, O., Redfern, S.A., Tyliszczak, T., Sadekov, A., Langer, G., Kimoto, K., Elderfield, H., 2013. The coordination of Mg in foraminiferal calcite. Earth Planet. Sci. Lett. 383, 134–141.
Bresson, C., Darolles, C., Carmona, A., Gautier, C., Sage, N., Roudeau, S., Ortega, R., Ansoborlo, E., Malard, V., 2013. Cobalt chloride speciation, mechanisms of cytotoxicity on human pulmonary cells, and synergistic toxicity with zinc. Metallomics 5, 133–143.
Bryan, S.P., Marchitto, T., 2010. Testing the utility of paleonutrient proxies Cd/Ca and Zn/Ca in benthic foraminifera from thermocline waters. Geochem. Geophys. Geosyst. 11, Q01005.
Callender, E., Rice, K.C., 2000. The urban environmental gradient: anthropogenic influences on the spatial and temporal distributions of lead and zinc in sediments. Environ. Sci. Technol. 34 (2), 232–238.
Cherchi, A., Da Pelo, S., Ibba, A., Mana, D., Buosi, C., Floris, N., 2009. Benthic foraminifera response and geochemical characterization of the coastal environment surrounding the polluted industrial area of Portovesme (South-Western Sardinia, Italy). Mar. Pollut. Bull. 59, 281–296.
Crutzen, P.J., 2002. Geology of mankind. Nature 415, 23.
Darke, S.A., Tyson, J.F., 1994. Review of solid sample introduction for plasma spectrometry and a comparison of results for laser ablation, electrothermal vaporization, and slurry nebulization. Microchem. J. 50, 310–336.
de Freita Prazeres, M., Martins, S.E., Bianchini, A., 2011. Biomarkers response to zinc exposure in the symbiont-bearing foraminifer *Amphistegina lessonii* (Amphisteginidae, Foraminifera). J. Exp. Mar. Biol. Ecol. 407, 116–121.
de Nooijer, L., Reichart, G.J., Dueñas-Bohórquez, A., Wolthers, M., Ernst, S., Mason, P., van Der Zwaan, G., 2007. Copper incorporation in foraminiferal calcite: results from culturing experiments. Biogeosciences 4, 493–504.
de Nooijer, L., Toyofuku, T., Kitazato, H., 2009. Foraminifera promote calcification by elevating their intracellular pH. Proc. Natl. Acad. Sci. U. S. A. 106, 15374–15378.
Debenay, J.P., Guillou, J.J., Geslin, E., Lesourd, M., Redois, F., 1998. Processus de cristallisation de plaquettes rhomboèdriques à la surface d'un test porcelané de foraminifère actuel. Geobios 31 (3), 295–302.
Díaz, S., Martín-González, A., Gutiérrez, J.C., 2006. Evaluation of heavy metal acute toxicity and bioaccumulation in soil ciliated protozoa. Environ. Int. 32, 711–717.
Dissard, D., Nehrke, G., Reichart, G.-J., Bijma, J., 2010. The impact of salinity on the Mg/Ca and Sr/Ca ratio in the benthic foraminifera *Ammonia tepida*: results from culture experiments. Geochim. Cosmochim. Acta 74, 928–940.
Eggins, S., De Deckker, P., Marshall, J., 2003. Mg/Ca variation in planktonic foraminifera tests: implications for reconstructing palaeo-seawater temperature and habitat migration. Earth Planet. Sc. Lett. 212, 291–306.
Eichler-Coelho, P.B., Duleba, W., Eichler, B.B., Coelho-Junior, C., 1996. Determinaçao do impacto ecologico do Valo Grande (Iguape, SP) a partir das associaçoes de foraminiferos e tecamebas. Rev. Bras. Biol. 57, 463–477.
Elzinga, E.J., Reeder, R.J., 2000. X-ray absorption spectroscopy study of Cu2 and Zn2 adsorption complexes at the calcite surface: implications for site-specific metal incorporation preferences during calcite crystal growth. Geochim. Cosmochim. Acta 66 (22), 3943–3954.
Ferraro, L., Sprovieri, M., Alberico, I., Lirer, F., Prevedello, L., Marsella, E., 2006. Benthic foraminifera and heavy metals distribution: a case study from the Naples Harbour (Tyrrhenian Sea, Southern Italy). Environ. Pollut. 142, 274–287.
Formigari, A., Irato, P., Santon, A., 2007. Zinc, antioxidants systems and metallothioneins in metal mediated-apoptosis: biochemical and cytochemical aspects. Comp. Biochem. Physiol. C 146, 443–459.
Foster, W.J., Armynot du Châtelet, E., Rogerson, M., 2012. Testing benthic foraminiferal distributions as a contemporary quantitative approach to biomonitoring estuarine heavy metal pollution. Mar. Pollut. Bull. 64, 1039–1048.
Frontalini, F., Coccioni, R., 2008. Benthic foraminifera for heavy metal pollution monitoring: a case study from the central Adriatic Sea coast of Italy. Estuar. Coast. Shelf Sci. 76, 404–417.
Geslin, E., Debenay, J.P., Duleba, W., Bonetti, C., 2002. Morphological abnormalities of foraminiferal tests in Brazilian environments: comparison between polluted and non-polluted areas. Mar. Micropaleontol. 45, 151–168.
Haake, F.W., 1971. Ultrastructures of miliolid walls. J. Foraminifer. Res. 1, 187–189.
Haase, H., Wätjen, W., Beyersmann, D., 2001. Zinc induces apoptosis that can be suppressed by lanthanum in C6 rat glioma cells. J. Biol. Chem. 382, 1227–1234.
Hathorne, E.C., Alard, O., James, R.H., Rogers, N.W., 2003. Determination of intratest variability of trace elements in foraminifera by laser ablation inductively coupled plasma-

mass spectrometry. Geochem. Geophys. Geosyst. 4 (12), 8408. http://dx.doi.org/10.1029/2003GC000539.
Hay, W.W., Towe, K.M., Wright, R.C., 1963. Ultramicrostructure of some selected foraminiferal tests. Micropaleontology 9, 171–175.
Hemleben, C., Anderson, O.R., Berthold, W., Spindler, M., 1986. Calcification and chamber formation in foraminifera-a brief overview. In: Leadbeater, B.S.C., Riding, R. (Eds.), Biomineralization in Lower Plants and Animals. Clarendon Press, Oxford, pp. 237–249.
Hintz, C.J., Shaw, T.J., Bernhard, J.M., Chandler, G.T., McCorkle, D.C., Blanks, J.K., 2006. Trace/minor element: calcium ratios in cultured benthic foraminifera. Part II: ontogenetic variation. Geochim. Cosmochim. Acta 70 (8), 1964–1976.
Hönisch, B., Hemming, N.G., 2005. Surface ocean pH response to variations in pCO_2 through two full glacial cycles. Earth Planet. Sci. Lett. 236, 305–314.
Katz, M., Cramer, B.S., Franzese, A., Hönisch, B., Miller, K.G., Rosenthal, Y., Wright, J.D., 2010. Traditional and emerging cheochemicla proxies in foraminifera. J. Foraminifer. Res. 40 (2), 165–192.
Langer, G., Gussone, N., Nehrke, G., Riesbell, U., Eisenhauer, A., Kuhnert, H., Rost, B., Trimborn, S., Thoms, S., 2006. Coccolith strontium to calcium ratios in *Emiliania huxleyi*: the dependence on seawater strontium and calcium concentrations. Limnol. Oceanogr. 51, 310–320.
Le Cadre, V., Debenay, J.-P., 2006. Morphological and cytological responses of *Ammonia* (foraminifera) to copper contamination: implication for the use of foraminifera as bioindicators of pollution. Environ. Pollut. 143, 304–317.
Levi, C., Labeyrie, L., Bassinot, F., Guichard, F., Cortijo, E., Waelbroeck, C., Caillon, N., Duprat, J., de Garidel-Thoron, T., Elderfield, H., 2007. Low-latitude hydrological cycle and rapid climate changes during the last deglaciation. Geochem. Geophys. Geosyst. 8, Q05N12. http://dx.doi.org/10.1029/2006GC001514.
Loeblich Jr., A.R., Tappan, H., 1964. Treatise on invertebrate paleontology. Part C, Protista 2. Sarcodinia chiefly "Thecamoebians" and Foraminiferida vol. 1. The Geological Society of America and The University of Kansas Press, p. 510.
Madkour, H.A., Ali, M.Y., 2009. Heavy metals in the benthic foraminifera from the coastal lagoons, Red Sea, Egypt: indicators of anthropogenic impact on environment (case study). Environ. Geol. 58, 543–553.
Marchitto, T.M., Curry, W.B., Oppo, D.W., 2000. Zinc concentrations in benthic foraminifera reflect seawater chemistry. Paleoceanography 15 (3), 299–306.
Mewes, A., Langer, G., de Nooijer, L., Bijma, J., Reichart, G.J., 2014. Effect of different seawater Mg^{2+} concentrations on calcification in two benthic foraminifers. Mar. Micropaleontol. 113, 56–64.
Montagna, P., McCulloch, M., Mazzoli, C., Silenzi, S., Odorico, R., 2007. The non-tropical coral *Cladocora caespitosa* as the new climate archive for the Mediterranean: high-resolution (weekly) trace element systematic. Quat. Sci. Rev. 26, 441–462.
Mucci, A., Morse, J.W., 1983. The incorporation of Mg^{2+} and Sr^{2+} into calcite overgrowths: influences of growth rate and solution composition. Geochim. Cosmochim. Acta 47, 217–233.
Munsel, D., Kramar, U., Dissard, D., Nehrke, G., Berner, Z., Bijma, J., Reichart, G.-J., Neumann, T., 2010. Heavy metal uptake in foraminiferal calcite: results of multi-element culture experiments. Biogeosciences 7, 2339–2350.
Nardelli, M.P., Sabbatini, A., Negri, A., 2013. Experimental chronic exposure of the foraminifer *Pseudotriloculina rotunda* to zinc. Acta Protozool. 52, 193–202.
Nehrke, G., Keul, N., Langer, G., de Nooijer, L.J., Bijma, J., Meibom, A., 2013. A new model for biomineralization and trace-element signatures of foraminifera tests. Biogeosciences 10, 6759–6767.
Raith, A., Hutton, R.C., Godfrey, J., 1996. Quantitation methods using laser ablation ICP-MS. Part 2: evaluation of new glass standards. Fresenius J. Anal. Chem. 354, 163–168.
Rathmann, S., Kuhnert, H., 2008. Carbonate ion effect on Mg/Ca, Sr/Ca and stable isotopes on the benthic foraminifera *Oridorsalis umbonatus* off Namibia. Mar. Micropaleontol. 66, 120–133.
Romano, E., Bergamin, L., Finoia, M.G., Carboni, M.G., Ausili, A., Gabellini, M., 2008. Industrial pollution at Bagnoli (Naples, Italy): benthic foraminifera as a tool in integrated programs of environmental characterisation. Mar. Pollut. Bull. 56, 439–457.
Sabbatini, A., Bassinot, F., Boussetta, S., Negri, A., Rebaubier, H., Dewilde, F., Nouet, J., Caillon, N., Morigi, C., 2011. Further constraints on the diagenetic influences and salinity effect on *Globigerinoides ruber* (white) Mg/Ca thermometry: implications in the Mediterranean Sea. Geochem. Geophys. Geosyst. 12, Q10005.
Samir, A., El-Din, A., 2001. Benthic foraminiferal assemblages and morphological abnormalities as pollution proxies in two Egyptian bays. Mar. Micropaleontol. 41, 193–227.
Schlumberger, C., 1893. Monographic des Miliolidées du Golfe de Marseille. Mémoires de la Société Zoologique de France 6, 199–224.
Schönfeld, J., Alve, E., Geslin, E., Jorissen, F., Korsun, S., Spezzaferri, S., FOBIMO, 2012. The FOBIMO (Foraminiferal BIo-MOnitoring) initiative – towards a standardised protocol for soft-bottom benthic foraminiferal monitoring studies. Mar. Micropaleontol. 94-95, 1–13.
Sharifi, A.R., Croudace, T.W., Austin, R.L., 1991. Benthonic foraminiferids as pollution indicators in Southampton water, Southern England, UK. J. Micropal. 10, 109–113.
Sousa, S.H.M., Duleba, W., Kfouri, P., Eichler, B.B., Furtado, V.V., 1997. Response of foraminiferal assemblages to environmental changes in the Sao Sebastiao Channel, Northern Coast of Sao Paulo State, Brazil. The First International Conference on Application of Micropaleontology in Environmental Sciences, Tel Aviv, Israel, pp. 109–110.
Stouff, V., Debenay, J.P., Lesourd, M., 1999. Origin of double and multiple tests in benthic foraminifera: observations in laboratory cultures. Mar. Micropaleontol. 36, 189–204.
Temmam, M., Paquette, J., Vali, H., 2000. Mn and Zn incorporation into calcite as a function of chloride aqueous concentration. Geochim. Cosmochim. Acta 64 (14), 2417–2430.
Towe, K.M., Cifelli, R., 1967. Wall ultrastructure in the calcareous foraminifera: crystallographic aspects and a model for calcification. J. Paleontol. 41, 742–762.
Valko, M., Morris, H., Cronin, M.T., 2005. Metals, toxicity and oxidative stress. Curr. Med. Chem. 12, 1161–1208.
Vénec-Peyré, M.T., 1981. Les foraminifères et la pollution: étude de la microfaune de la cale du Dourduff (embouchure de la rivière de Morlaix). Cah. Biol. Mar. 25–33.
Vénec-Peyré, M.T., Lipps, J.H., Weber, M., Bartolini, A., 2010. Amoco Cadiz oil spill and Foraminifera thirty years later. FORAMS 2010 (International Symposium on Foraminifera), p. 193 (Abstract Volume).
Wuana, R.A., Okieimen, F.E., 2011. Heavy metals in contaminated soils: a review of sources, chemistry, risks and best available strategies for remediation. ISRN Ecol. (ID 402647).
Yanko, V., Ahmad, M., Kaminski, M., 1998. Morphological deformities of benthic foraminiferal tests in response to pollution by heavy metal: implications for pollution monitoring. J. Foraminifer. Res. 28, 177–200.
Zalasiewicz, J., Williams, M., Haywood, A., Ellis, M., 2011. The Anthropocene: a new epoch of geological time? Phil. Trans. R. Soc. A 369, 835–841.

Appendix A

A.1 Setting of LA experimental conditions

Due to the particular calcite structure and chamber arrangement of *P. rotunda,* it was compulsory to find the best ablation parameters to prevent chamber destruction and the ablation of the innermost (older) chambers. Miliolid foraminifera can react very differently from rotaliids that are more often analyzed in the existing literature. Thus, several parameters, such as the area to ablate, beam intensity, frequency, and duration (Tab. A.1) had to be carefully set and combined. Several preliminary tests were therefore performed.

Tab. A.1 brief description of the configuration parameters of the instrument

Laser intensity (%). It is the percentage of the laser beam that reaches the sample surface; the lasers beam is characterized by a sort of cavity where the photons make many circuits between two reflective ends. The effective number of photons exiting that cavity (i.e., laser intensity) can be modulated changing the geometry of the reflective ends.
Laser frequency (Hz). It is the time during which the laser output pulse power remains continuously above half its maximum value.
Laser fluency (J/cm^2). It is the energy delivered per unit area; it depends not only on laser features, but also on sample chemical and physical properties. This parameter could not be pre-set, but is measured during ablation.
Duration(s) and scan-speed. It is the time of persistence of the laser ablation on the ablating surface. When ablation is done following a line, it is possible to choose whether to use the same time for different lengths, or vary the time (i.e., scan-speed) depending on the length you intend to ablate.
Purging gas flow (argon, mL/min). It is the volume of gas used to transport the ablated sample to plasma. We take this parameter always constant at 500mL/min.

Before starting optimization of laser parameters it was assumed that:

i) Linear ablation with proper width should be preferred to spot ablation in order to sample a greater volume, reducing therefore errors of low counting due to relatively low expected zinc concentrations and/or possibly patchy distribution of zinc into the shell.

ii) Pre-ablation can be a good method to clean miliolid foraminiferal surface from potential contaminations (e.g. organic matter derived from culture feeding of organisms, potential residuals of salt from artificial seawater, etc.), before data acquisition.

Several trials on foraminiferal sample-tests were then made varying laser parameter in order to find their most suitable values and combinations; after each trial, samples were observed via ESEM to check for the obtained results. Hereafter are reported some example of the tests we performed. High laser intensity (<50%) and frequency (<4Hz) result in partial or total destruction of the shell chambers (Fig. A.1a), ablation of the innermost chambers and/or partial destruction of chamber (Fig. A.1b). No negative effects due to higher duration times were apparently noticed. An example of optimized ablation is reported in figure A.1c obtained setting ablation parameters as reported in table 1 (main text).

An intriguing problem, to our knowledge never discussed in literature, is the distance between the laser source and the sample, estimated and set through an optical focusing system. One may speculate that the focus is uniquely determined and, thus, should not influence repeatability of measurements. However, this may possibly be true only for perfectly flat samples, not the foraminifera used in this study, characterized by a shell curvature varying both inside the same specimen and from specimen to specimen. The high possibility of laser modulation enables ablation only on the chamber of interest. Keeping constant the length of the ablation line throughout the

whole experimental section, and given also the small size of the specimens, the error introduced by a different curvature is, in our opinion, negligible.

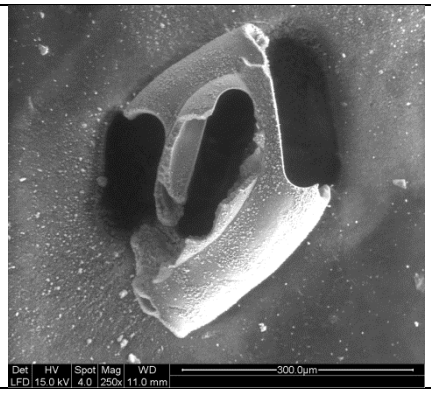

Fig. A.1a. Laser intensity 100%; Laser frequency 10Hz: total destruction of the chamber

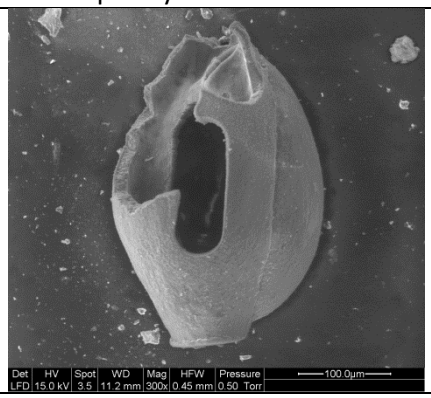

Fig. A.1b. Laser intensity 75%; Laser frequency 6Hz: partial destruction of the chamber and ablation of the innermost chambers

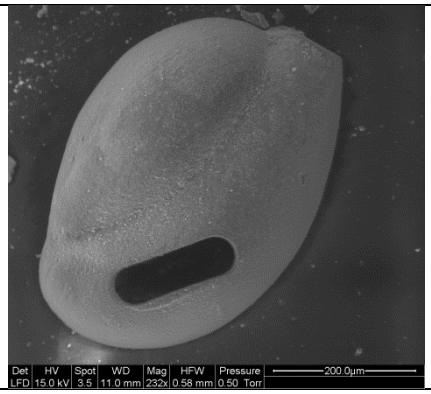

Fig. A.1c. Laser intensity 50%; Laser frequency 4Hz: optimized ablation

Tab. A.2. Zn and Ca concentration in the first formed chamber of foraminifera shell in water at variable Zn concentration. $D_{Zn}=[(Zn/Ca)_{calcite}]/[(Zn/Ca)_{seawater}]$; u.d.l.= under detection limit. Zn and Ca concentration values are also reported for passive incorporation test. NIST610 certified standard and glue used to fix foraminifera to sample holder were also measured.

Sample of foraminiferal calcite	Zn mol/Kg	Ca mol/Kg	Zn/Ca mmol/mol	D_{Zn}
Sea water				
S1-sea	0.011	10.014	1.131	4.065
S2-sea	0.011	9.984	1.110	3.989
S3-sea	0.011	10.026	1.144	4.113
S4-sea	0.011	9.961	1.130	4.063
S5-sea	0.011	10.019	1.112	3.999
S6-sea	0.011	10.031	1.108	3.981
S7-sea	0.011	10.034	1.098	3.947
S8-sea	0.011	10.046	1.134	4.078
S9-sea	0.011	10.021	1.142	4.104
S10-sea	0.011	10.051	1.132	4.069
S11-sea	0.011	10.054	1.103	3.965
Mean	*0.011*	*10.022*	*1.122*	*4.034*
Stand. Dev.	*0.000*	*0.028*	*0.016*	*0.059*
Zn addition: 0.01mg/L				
S1-sea+0.01	0.012	9.981	1.165	3.925
S2-sea+0.01	0.012	10.024	1.165	3.926
S3-sea+0.01	0.011	9.984	1.142	3.848
S4-sea+0.01	0.011	9.991	1.145	3.857
S5-sea+0.01	0.011	10.029	1.141	3.845
Mean	*0.012*	*10.002*	*1.152*	*3.880*
Stand. Dev.	*0.000*	*0.023*	*0.012*	*0.042*
Zn addition: 0.1mg/L				
S1-sea+0.1	0.012	9.969	1.227	2.640
S2-sea+0.1	0.012	10.021	1.225	2.634
S3-sea+0.1	0.012	9.939	1.211	2.606
S4-sea+0.1	0.012	10.076	1.217	2.618
S5-sea+0.1	0.012	10.026	1.217	2.618
S6-sea+0.1	0.012	10.019	1.193	2.567
S7-sea+0.1	0.012	10.054	1.221	2.627
S8-sea+0.1	0.012	9.936	1.231	2.648
S9-sea+0.1	0.012	9.996	1.205	2.592
S10-sea+0.1	0.012	10.059	1.215	2.614
Mean	*0.012*	*10.009*	*1.216*	*2.616*
Stand. Dev.	*0.000*	*0.049*	*0.011*	*0.024*

Zn addition: 1mg/L	Zn mol/Kg	Ca mol/Kg	Zn/Ca mmol/mol	D_{Zn}
S1-sea+1.0	0.017	10.076	1.724	0.804
S2-sea+1.0	0.018	9.939	1.810	0.844
S3-sea+1.0	0.017	9.909	1.755	0.818
S4-sea+1.0	0.018	9.944	1.795	0.837
S5-sea+1.0	0.018	9.919	1.795	0.837
S6-sea+1.0	0.017	10.076	1.729	0.806
S7-sea+1.0	0.018	10.026	1.752	0.816
S8-sea+1.0	0.018	10.039	1.746	0.814
S9-sea+1.0	0.018	10.001	1.766	0.823
S10-sea+1.0	0.019	10.076	1.840	0.858
Mean	*0.018*	*10.000*	*1.771*	*0.826*
Stand. Dev.	*0.000*	*0.068*	*0.037*	0.017
Zn addition: 10mg/L				
S1-sea+10	0.041	10.006	4.066	0.215
S2-sea+10	0.039	10.168	3.880	0.205
S3-sea+10	0.038	10.091	3.742	0.198
S4-sea+10	0.041	10.056	4.067	0.215
S5-sea+10	0.038	10.006	3.832	0.202
S6-sea+10	0.036	10.093	3.547	0.187
S7-sea+10	0.037	10.046	3.688	0.195
S8-sea+10	0.037	10.006	3.724	0.197
S9-sea+10	0.038	10.073	3.771	0.199
Mean	*0.038*	*10.061*	*3.813*	*0.201*
Stand. Dev.	*0.002*	*0.053*	*0.171*	*0.009*
Passive sorption test				
S1-empty+10	0.012	9.870	1.179	
S2-empty+10	0.012	9.875	1.160	
Mean	0.012	9.873	1.170	
Stand. Dev.	0.000	0.004	0.014	
Standards & Sample holder				
SampleHold	udl	0.001		
NIST610-611	0.007	2.141		
Samples of seawater	Zn mol/L	Ca mol/L	Zn/Ca mmol/mol	
sea	2.279E-06	8.191E-03	0.278	
sea+0.01	2.432E-06	8.191E-03	0.297	
sea+0.10	3.808E-06	8.191E-03	0.465	
sea+1.0	1.757E-05	8.191E-03	2.145	
sea+10	1.552E-04	8.191E-03	18.948	